SUPPORTING INFORMATION

Incorporation of hexacyanidoferrate(III) ion in photoluminescent trimetallic Eu(3-pyridone)[$Co_{1-x}Fe_x(CN)_6$] chains exhibiting tunable visible light absorption and emission properties

Szymon Chorazy,[a] Jakub J. Zakrzewski,[a] Junhao Wang,[b] Shin-ichi Ohkoshi,[b] and Barbara Sieklucka*[a]*

[a]Faculty of Chemistry, Jagiellonian University, Gronostajowa 2, 30-387 Krakow, Poland. [b]Department of Chemistry, School of Science, The University of Tokyo, 7-3-1 Hongo, Bunkyo-ku, Tokyo 113-0033, Japan.

*Corresponding authors: chorazy@chemia.uj.edu.pl; barbara.sieklucka@uj.edu.pl

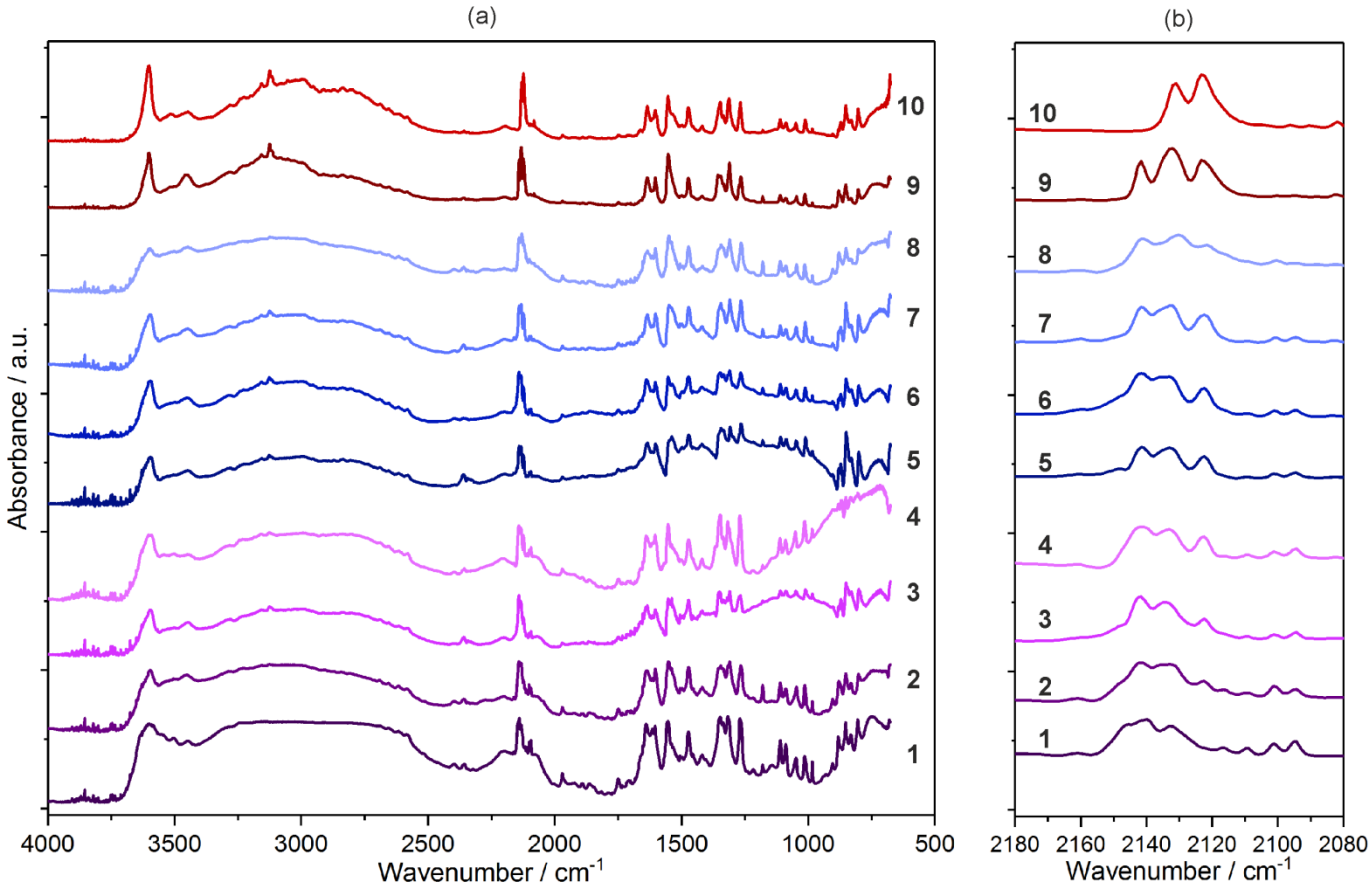

Figure S1. Infrared absorption spectra of **1–10** in the range of 4000–700 cm^{-1} (*a*), and the limited range of 2180–2080 cm^{-1}, related to the stretching vibrations of cyanide ligands (*b*).[S1]

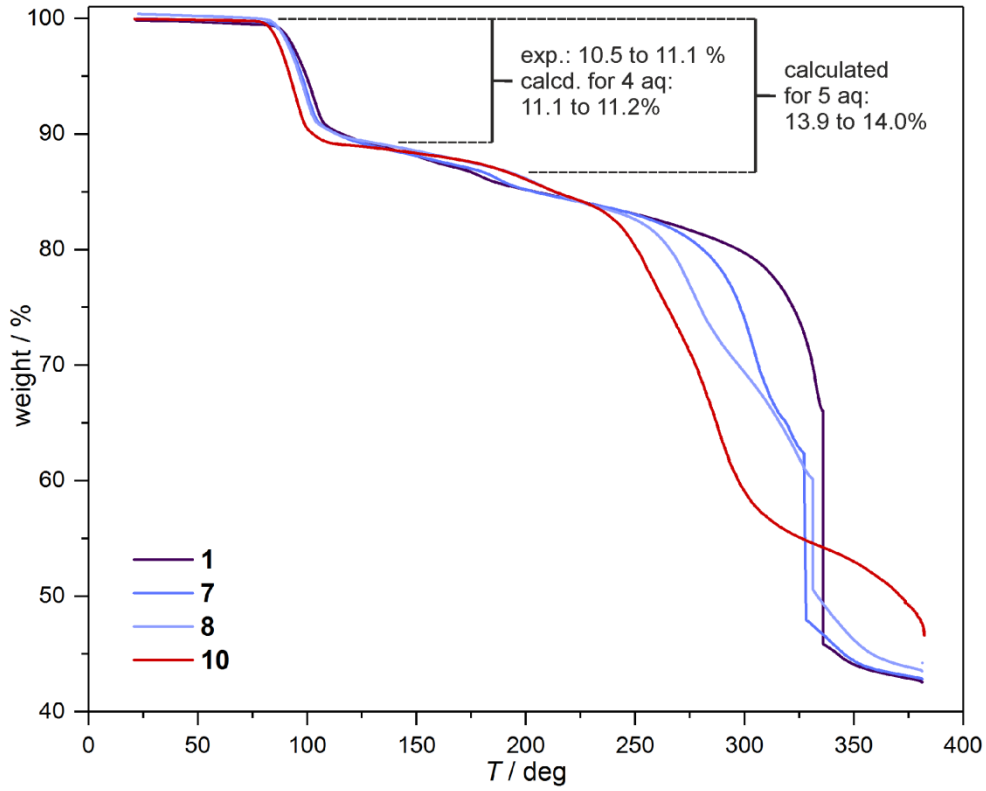

Figure S2. Thermogravimetric curves of **1**, **7**, **8**, and **10** collected in the temperature range of 20–375 °C. The steps related to the loss of water molecules were depicted (see the comment below for details). The experiments were conducted under an air atmosphere with the heating rate of 1 °C per minute.

Comment to Figure S2

Upon heating under an air atmosphere, the powder samples of **1**, **7**, **8**, and **10** show the stable composition up to ca. 80–90 °C. Among these compounds, Eu/Fe-containing **10** reveals the lowest thermal stability up to 80 °C, while the highest thermal stability to almost 90 °C is characteristic of Eu/Co-containing **1**. The mixed Eu/Co/Fe compounds, **7** and **8** exhibit the intermediate thermal stability to ca. 83–86 °C. Further heating leads to the significant and rapid decrease of the mass of the samples in the relatively narrow range of 90–120 °C. The related decreases of the mass are similar in all the investigated compounds, 10.5% for **1**, 10.6% for **7** and **8**, up to 11.1% for **10**. These values correspond well to the mass loss of 11.1–11.2% expected for the removal of four water molecules per one {EuM} (M = Co, Fe) unit. It indicates that, at ca. 120 °C, **1**, **7**, **8**, and **10** undergo the phase transition to the partially dehydrated $\{[Eu^{III}(3\text{-pyridone})_2(H_2O)][M^{III}(CN)_6]\}$ (Ln = Co, Fe) form with a small amount of remaining water molecules. This last portion of water is gradually removing on further heating in the much broader temperature range from 120 °C to 190–200 °C. Thus, at ca. 200 °C all the samples are expected to reach the fully dehydrated form of $\{[Eu^{III}(3\text{-pyridone})_2][M^{III}(CN)_6]\}$ (Ln = Co, Fe). At higher temperatures, the further decrease of the mass is observed, and it can be ascribed to the removal of terminal cyanides and/or gradual decomposition of 3-pyridone ligands.[S2] The related dramatic decrease of the sample's mass is observed below 240, 260, 270, and 300 °C for **1**, **7**, **8**, and **10**, respectively. It shows the highest thermal stability for Eu/Co-containing **1**, and the decrease of thermal stability occurring with the increasing amount of Fe^{III} within the coordination network.

Table S1. Crystal data and structure refinement for **1**, **2**, and **3**.

Compound		**1**	**2**	**3**
formula		$Eu_1Co_1C_{16}H_{20}N_8O_7$	$Eu_1Co_{0.97}Fe_{0.03}C_{16}H_{20}N_8O_7$	$Eu_1Co_{0.94}Fe_{0.06}C_{16}H_{20}N_8O_7$
formula weight / g·mol^{-1}		647.29	647.2	647.1
T / K		298(2)		
λ / Å		0.71073		
crystal system		monoclinic		
space group		*C* 2/c (no. 15)		
unit cell	*a* / Å	15.9157(5)	15.869(4)	15.922(3)
	b / Å	9.2572(3)	9.274(3)	9.2557(15)
	c / Å	17.7350(6)	17.720(7)	17.732(3)
	β / deg	116.5470(10)	116.259(10)	116.446(6)
volume / Å^3		**2337.49(13)**	**2338.50(13)**	**2339.7(7)**
Z		4	4	4
calculated density / g·cm^{-3}		1.839	1.838	1.837
absorption coefficient / cm^{-1}		3.421	3.417	3.412
F(000)		1272	1272	1272
crystal size / mm × mm × mm		0.22 × 0.14 × 0.06	0.34 × 0.30 × 0.30	0.17 × 0.15 × 0.11
crystal type		colourless block	yellow block	orange block
Θ range / deg		2.568–28.796	2.563–26.018	2.566–26.731
limiting indices		-21 < *h* < 21 -12 < *k* < 12 -23 < *l* < 23	-19 < *h* < 19 -11 < *k* < 6 -21 < *l* < 16	-20 < *h* < 16 -11 < *k* < 11 -22 < *l* < 22
collected reflections		14042	4046	8078
unique reflections		3036	2294	2492
R_{int}		0.0223	0.0135	0.0215
completeness		0.995	0.994	1.000
max. and min. transmission		0.520 and 0.821	0.39 and 0.427	0.595 and 0.705
data/restraints/parameters		3036/5/182	2294/5/182	2492/5/182
GOF on F^2		1.243	1.348	1.028
final *R* indices		R_1 = 0.0168 [I>2σ(I)] wR_2 = 0.0503 (all data)	R_1 = 0.0271 [I>2σ(I)] wR_2 = 0.0751 (all data)	R_1 = 0.0172 [I>2σ(I)] wR_2 = 0.043 (all data)
largest diffraction peak/hole		0.548/-1.012 e·Å^{-3}	0.68/-2.389 e·Å^{-3}	0.353/-0.757 e·Å^{-3}

Table S2. Crystal data and structure refinement for **4**, **5**, and **6**.

Compound		**4**	**5**	**6**
formula		$Eu_1Co_{0.91}Fe_{0.09}C_{16}H_{20}N_8O_7$	$Eu_1Co_{0.88}Fe_{0.12}C_{16}H_{20}N_8O_7$	$Eu_1Co_{0.85}Fe_{0.15}C_{16}H_{20}N_8O_7$
formula weight / g·mol^{-1}		647.01	646.92	646.83
T / K		298(2)		
λ / Å		0.71073		
crystal system		monoclinic		
space group		C 2/c (no. 15)		
unit cell	a / Å	15.907(3)	15.9056(18)	15.9088(10)
	b / Å	9.268(2)	9.2580(11)	9.2677(6)
	c / Å	17.718(4)	17.746(2)	17.7418(16)
	β / deg	116.505(4)	116.540(4)	116.514(2)
volume / Å^3		**2337.4(9)**	**2337.8(5)**	**2340.7(3)**
Z		4	4	4
calculated density / g·cm^{-3}		1.839	1.838	1.835
absorption coefficient / cm^{-1}		3.413	3.410	3.403
F(000)		1272	1272	1271
crystal size / mm × mm × mm		0.19 × 0.18 × 0.07	0.24 × 0.15 × 0.09	0.18 × 0.12 × 0.04
crystal type		orange block	orange block	orange block
Θ range / deg		2.622–25.027	2.566–27.103	2.566–27.103
limiting indices		$-18 < h < 18$ $-10 < k < 11$ $-19 < l < 21$	$-20 < h < 20$ $-11 < k < 11$ $-22 < l < 22$	$-20 < h < 20$ $-11 < k < 11$ $-22 < l < 22$
collected reflections		4999	12942	12873
unique reflections		2004	2583	2586
R_{int}		0.0165	0.0265	0.0284
completeness		0.976	1.000	1.000
max. and min. transmission		0.563 and 0.796	0.495 and 0.749	0.579 and 0.876
data/restraints/parameters		2004/5/182	2583/5/182	2586/5/182
GOF on F^2		1.026	1.013	1.100
final R indices		R_1 = 0.0155 [I>2σ(I)] wR_2 = 0.0394 (all data)	R_1 = 0.0157 [I>2σ(I)] wR_2 = 0.039 (all data)	R_1 = 0.017 [I>2σ(I)] wR_2 = 0.0438 (all data)
largest diffraction peak/hole		0.395/-0.488 e·Å^{-3}	0.409/-0.535 e·Å^{-3}	0.332/-0.646 e·Å^{-3}

Table S3. Crystal data and structure refinement for **7**, **8**, **9**, and **10**.

Compound		**7**	**8**	**9**	**10**
formula		$Eu_1Co_{0.25}Fe_{0.75}C_{16}H_{20}N_8O_7$	$Eu_1Co_{0.5}Fe_{0.5}C_{16}H_{20}N_8O_7$	$Eu_1Co_{0.25}Fe_{0.75}C_{16}H_{20}N_8O_7$	$Eu_1Fe_1C_{16}H_{20}N_8O_7$
formula weight / $g \cdot mol^{-1}$		646.52	645.75	644.98	644.21
T / K		298(2)			
λ / Å		0.71073			
crystal system		monoclinic			
space group		C 2/c (no. 15)			
unit cell	a / Å	15.9161(15)	15.9139(7)	15.914(2)	15.9155(18)
	b / Å	9.2678(8)	9.2609(4)	9.2658(11)	9.2628(11)
	c / Å	17.7480(16)	17.7694(8)	17.800(2)	17.822(2)
	β / deg	116.527(3)	116.4190(10)	116.489(5)	116.366(3)
volume / Å^3		**2342.3(4)**	**2345.30(18)**	**2349.1(5)**	**2354.1(5)**
Z		4	4	4	4
calculated density / $g \cdot cm^{-3}$		1.833	1.829	1.824	1.818
absorption coefficient / cm^{-1}		3.392	3.365	3.338	3.308
F(000)		1271	1270	1269	1268
crystal size / mm × mm × mm		0.19 × 0.10 × 0.08	0.13 × 0.09 × 0.08	0.16 × 0.13 × 0.08	0.18 × 0.14 × 0.09
crystal type		orange block	orange block	orange block	red block
Θ range / deg		2.622–27.144	2.623–27.176	2.557–27.103	2.551–27.225
limiting indices		$-20 < h < 20$ $-11 < k < 11$ $-22 < l < 22$	$-20 < h < 20$ $-11 < k < 11$ $-22 < l < 22$	$-20 < h < 17$ $-11 < k < 9$ $-22 < l < 22$	$-20 < h < 20$ $-11 < k < 11$ $-22 < l < 22$
collected reflections		12812	12941	6244	12892
unique reflections		2588	2604	2588	2612
R_{int}		0.0244	0.0221	0.0204	0.0218
completeness		0.997	0.998	0.996	0.994
max. and min. transmission		0.563 and 0.773	0.669 and 0.775	0.617 and 0.776	0.587 and 0.755
data/restraints/ parameters		2588/5/182	2604/5/182	2588/5/182	2612/10/182
GOF on F^2		1.094	1.117	1.070	1.475
final R indices		R_1 = 0.0150 [I>2σ(I)] wR_2 = 0.0351 (all data)	R_1 = 0.0156 [I>2σ(I)] wR_2 = 0.0377 (all data)	R_1 = 0.0193 [I>2σ(I)] wR_2 = 0.0465 (all data)	R_1 = 0.0181 [I>2σ(I)] wR_2 = 0.1044 (all data)
largest diffraction peak/hole		0.370/-0.526 $e \cdot Å^{-3}$	0.320/-0.656 $e \cdot Å^{-3}$	0.366/-0.728 $e \cdot Å^{-3}$	1.003/-2.301 $e \cdot Å^{-3}$

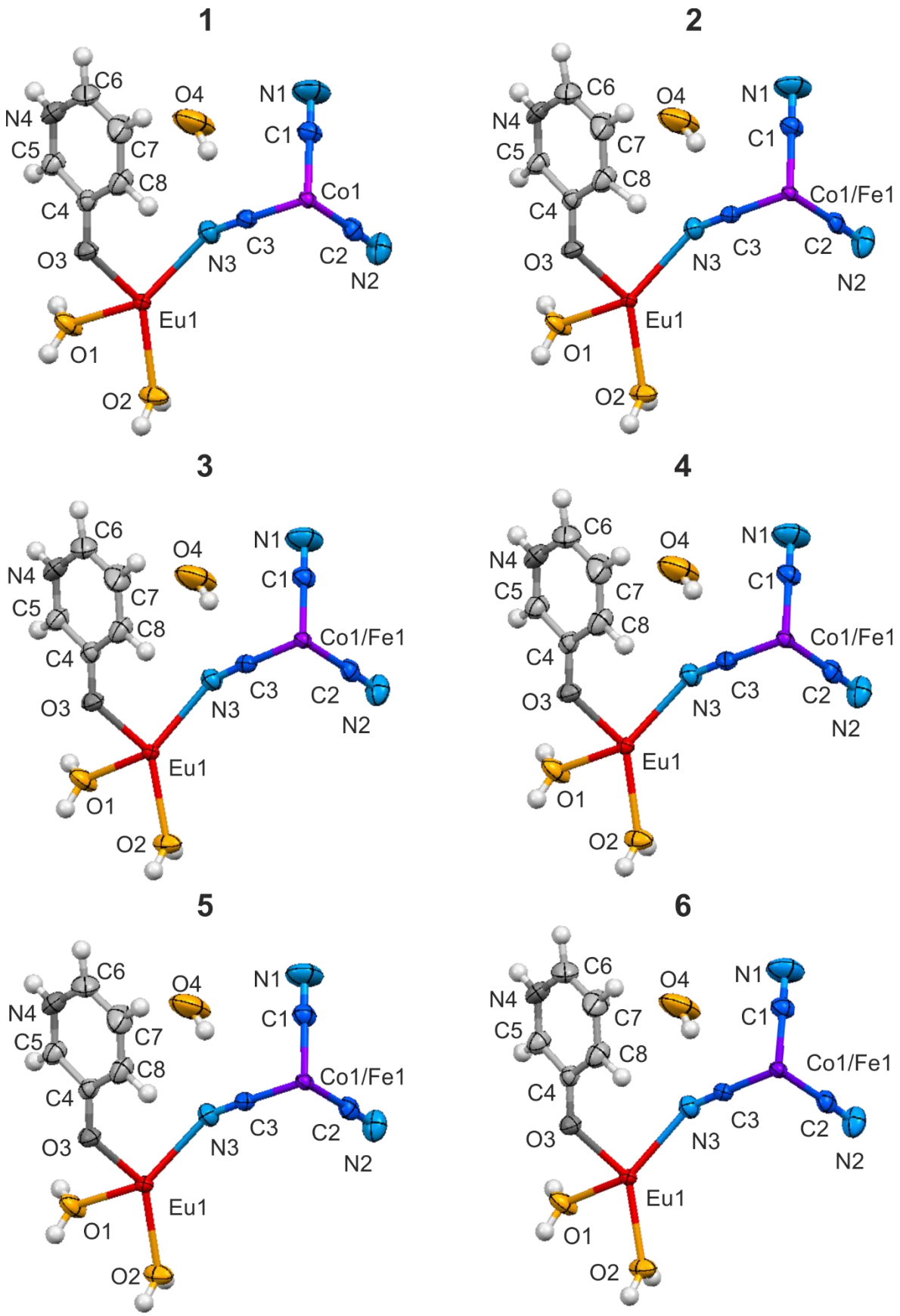

Figure S3. Comparison of the asymmetric units of **1**–**6** with the atoms labelling schemes. Thermal ellipsoids are presented at the 70% probability level. The related bond lengths and angles are collected in Tables S1–S2.

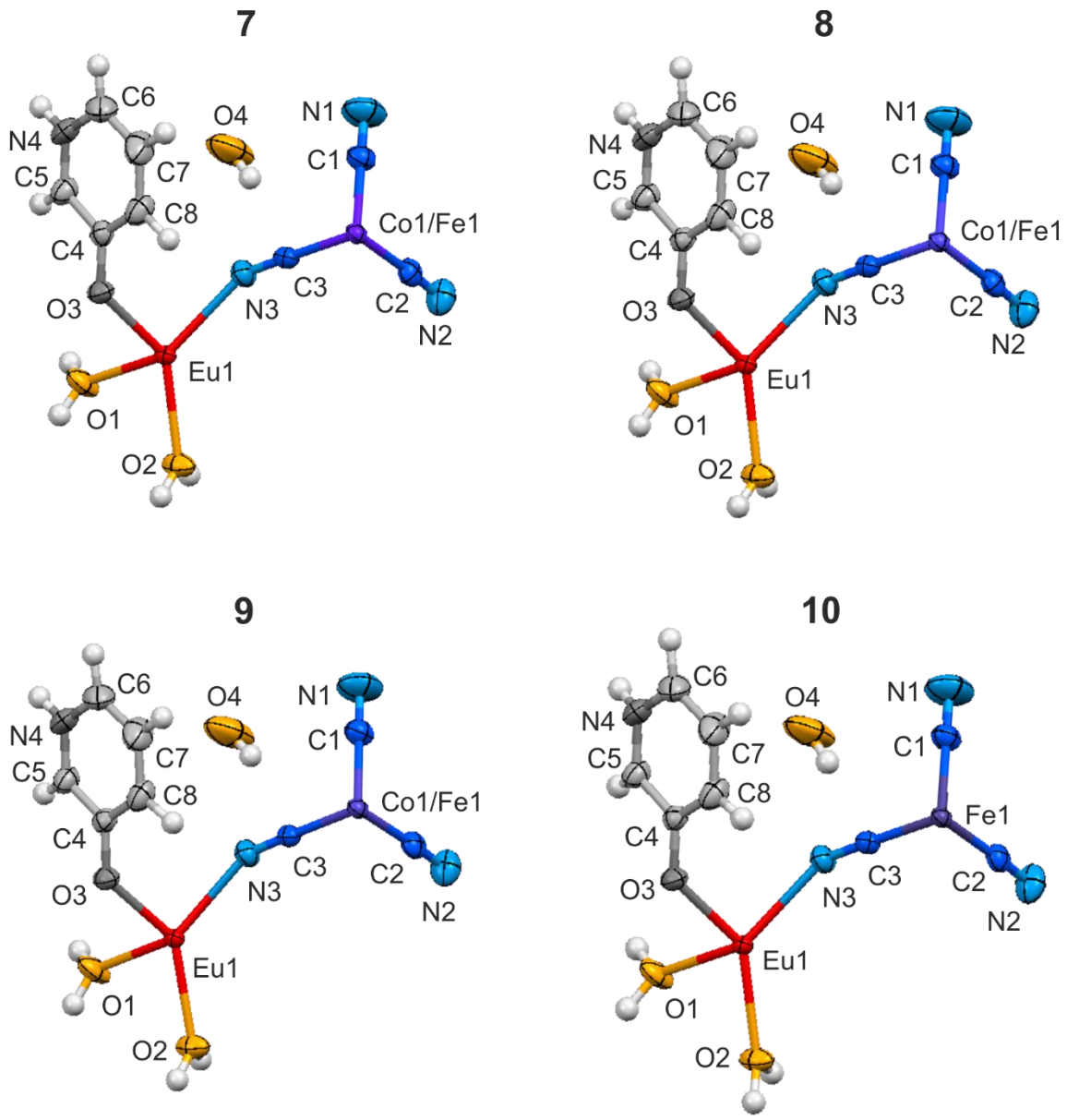

Figure S4. Comparison of the asymmetric units of **7**–**10** with the atoms labelling schemes. Thermal ellipsoids are presented at the 70% probability level. The related bond lengths and angles are collected in Table S3.

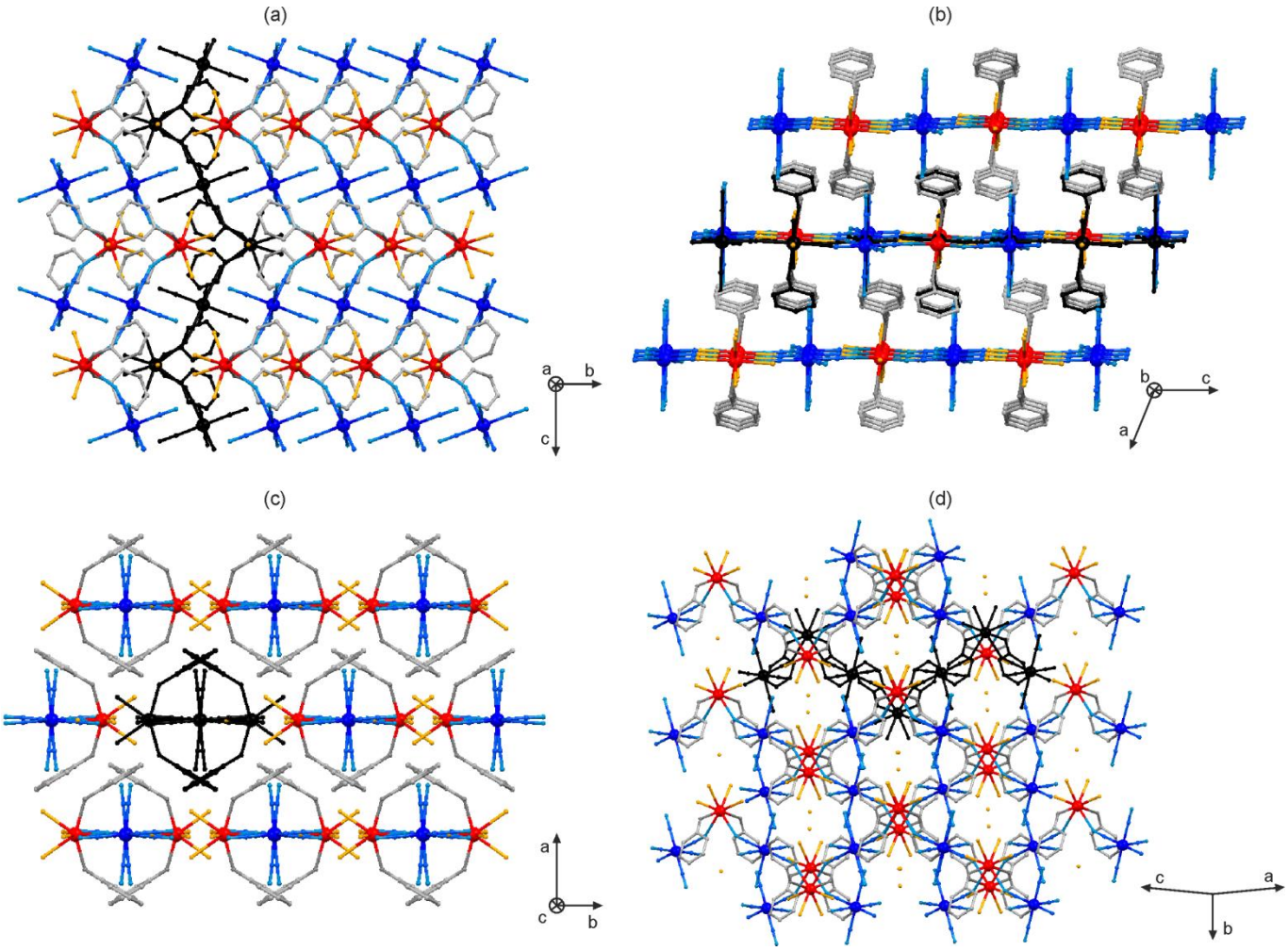

Figure S5. The supramolecular arrangement of the cyanido-bridged chains and crystallization water molecules of **8** presented along the crystallographic ***a*** axis (*a*), ***b*** axis (*b*), ***c*** axis (*c*), and the [101] direction (*d*). One representative chain was shown using black colour.

Table S4. Detailed structure parameters of **1**, **2**, and **3**.

Details of $[M^{III}(CN)_6]^{3-}$ complexes			
Parameter	**1** (M = Co)	**2** (M = $Co_{0.97}Fe_{0.03}$)	**3** (M = $Co_{0.94}Fe_{0.06}$)
M1–C1	1.900(2) Å	1.910(4) Å	1.903(2) Å
M1–C2	1.905(2) Å	1.902(3) Å	1.910(2) Å
M1–C3	1.8988(19) Å	1.897(3) Å	1.901(2) Å
C1–N1	1.138(3) Å	1.134(5) Å	1.135(3) Å
C2–N2	1.142(3) Å	1.143(5) Å	1.149(3) Å
C3–N3	1.144(3) Å	1.147(4) Å	1.145(3) Å
M1–C1–N1	178.3(3)°	178.5(4)°	178.2(3)°
M1–C2–N2	177.8(2)°	178.0(3)°	178.1(2)°
M1–C3–N3	177.17(18)°	177.3(3)°	177.4(2)°
C1–M1–C2	89.39(9)°	89.56(15)°	89.39(10)°
C1–M1–C3	89.67(9)°	89.49(14)°	89.72(9)°
C2–M1–C3	89.23(8)°	89.49(14)°	89.16(9)°
M1–Eu1 distance	5.444 Å	5.444 Å	5.443 Å
Details of $[Eu^{III}(3\text{-pyridone})_2(H_2O)_4(NC)_2]^{+}$ complexes			
Parameter	**1** (M = Co)	**2** (M = $Co_{0.97}Fe_{0.03}$)	**3** (M = $Co_{0.94}Fe_{0.06}$)
Eu1–N3	2.5728(18) Å	2.573(3) Å	2.5697(19) Å
Eu1–O1	2.4324(16) Å	2.429(3) Å	2.4312(18) Å
Eu1–O2	2.4641(15) Å	2.466(2) Å	2.4639(17) Å
Eu1–O3	2.2974(14) Å	2.295(2) Å	2.2997(16) Å
Eu1–N3–C3	152.92(16)°	152.6(3)°	152.93(17)°
Eu1–O3–C4	134.34(13)°	134.3(2)°	134.31(14)°
N3–Eu1–N3	78.56(9)°	78.19(14)°	78.41(9)°
O1–Eu1–O1	144.04(8)°	144.04(12)°	144.22(8)°
O2–Eu1–O2	70.61(7)°	70.50(12)°	70.67(8)°
O3–Eu1–O3	149.49(7)°	149.32(12)°	149.62(8)°
N3–Eu1–O1	68.70(6)° 147.26(6)°	68.89(9)° 147.08(9)°	68.68(6)° 147.09(6)°
N3–Eu1–O2	127.53(6)° 130.86(6)°	127.50(9)° 131.22(9)°	127.61(6)° 130.84(6)°
N3–Eu1–O3	75.28(6)° 81.18(6)°	75.42(9)° 80.85(9)°	75.29(6)° 81.24(6)°
O1–Eu1–O2	73.27(6)° 77.53(6)°	73.05(9)° 77.72(9)°	73.30(6)° 77.65(6)°
O1–Eu1–O3	90.52(6)° 98.82(6)°	90.83(10)° 98.56(10)°	90.59(7)° 98.67(7)°
O2–Eu1–O3	70.31(5)° 140.04(5)°	70.45(8)° 140.06(8)°	70.20(6)° 140.02(6)°

Table S5. Detailed structure parameters of **4**, **5**, and **6**.

Details of $[M^{III}(CN)_6]^{3-}$ complexes			
Parameter	**4** (M = $Co_{0.91}Fe_{0.09}$)	**5** (M = $Co_{0.88}Fe_{0.12}$)	**6** (M = $Co_{0.85}Fe_{0.15}$)
M1–C1	1.904(2) Å	1.905(2) Å	1.907(2) Å
M1–C2	1.911(2) Å	1.909(2) Å	1.914(2) Å
M1–C3	1.901(2) Å	1.9045(19) Å	1.905(2) Å
C1–N1	1.141(3) Å	1.138(3) Å	1.138(3) Å
C2–N2	1.141(3) Å	1.143(3) Å	1.140(3) Å
C3–N3	1.145(3) Å	1.147(3) Å	1.145(3) Å
M1–C1–N1	178.7(3)°	178.3(2)°	178.4(3)°
M1–C2–N2	178.1(2)°	178.1(2)°	178.1(2)°
M1–C3–N3	177.3(2)°	177.15(18)°	177.3(2)°
C1–M1–C2	89.36(10)°	89.42(9)°	89.30(10)°
C1–M1–C3	89.50(9)°	89.67(8)°	89.62(9)°
C2–M1–C3	89.28(9)°	89.24(8)°	89.19(9)°
M1–Eu1 distance	5.443 Å	5.446 Å	5.447 Å
Details of $[Eu^{III}(3\text{-pyridone})_2(H_2O)_4(NC)_2]^{+}$ complexes			
Parameter	**4** (M = $Co_{0.91}Fe_{0.09}$)	**5** (M = $Co_{0.88}Fe_{0.12}$)	**6** (M = $Co_{0.85}Fe_{0.15}$)
Eu1–N3	2.568(2) Å	2.5675(17) Å	2.5697(19) Å
Eu1–O1	2.4276(19) Å	2.4291(15) Å	2.4301(17) Å
Eu1–O2	2.4634(17) Å	2.4627(15) Å	2.4634(17) Å
Eu1–O3	2.2970(16) Å	2.2958(14) Å	2.2996(16) Å
Eu1–N3–C3	152.82(17)°	152.93(16)°	152.81(17)°
Eu1–O3–C4	134.38(13)°	134.20(12)°	134.20(14)°
N3–Eu1–N3	78.32(9)°	78.46(8)°	78.39(9)°
O1–Eu1–O1	144.10(8)°	144.18(8)°	144.13(8)°
O2–Eu1–O2	70.41(8)°	70.39(7)°	70.43(8)°
O3–Eu1–O3	149.35(8)°	149.60(7)°	149.42(8)°
N3–Eu1–O1	68.79(6)° 147.11(6)°	68.68(5)° 147.14(6)°	68.74(6)° 147.13(6)°
N3–Eu1–O2	127.69(7)° 130.98(6)°	127.68(6)° 130.90(6)°	127.61(6)° 131.00(6)°
N3–Eu1–O3	75.28(6)° 81.04(6)°	75.32(5)° 81.21(5)°	75.27(6)° 81.11(6)°
O1–Eu1–O2	73.27(6)° 77.54(7)°	73.35(6)° 77.52(6)°	73.26(6)° 77.58(6)°
O1–Eu1–O3	90.69(7)° 98.68(7)°	90.51(6)° 98.77(6)°	90.54(6)° 98.80(6)°
O2–Eu1–O3	70.46(6)° 140.03(6)°	70.35(5)° 139.89(5)°	70.43(6)° 139.98(6)°

Table S6. Detailed structure parameters of **7**, **8**, **9** and **10**.

Details of $[M^{III}(CN)_6]^{3-}$ complexes				
Parameter	**7** (M = $Co_{0.75}Fe_{0.25}$)	**8** (M = $Co_{0.5}Fe_{0.5}$)	**9** (M = $Co_{0.25}Fe_{0.75}$)	**10** (M = Fe)
M1–C1	1.9100(19) Å	1.922(2) Å	1.932(3) Å	1.941(4) Å
M1–C2	1.917(2) Å	1.925(2) Å	1.934(3) Å	1.940(4) Å
M1–C3	1.9081(18) Å	1.9180(18) Å	1.927(2) Å	1.929(3) Å
C1–N1	1.140(3) Å	1.133(3) Å	1.136(3) Å	1.125(6) Å
C2–N2	1.145(3) Å	1.145(3) Å	1.145(3) Å	1.139(5) Å
C3–N3	1.147(2) Å	1.144(2) Å	1.143(3) Å	1.146(5) Å
M1–C1–N1	178.4(2)°	178.1(2)°	178.3(3)°	178.3(5)°
M1–C2–N2	177.85(19)°	177.90(19)°	178.0(2)°	177.7(4)°
M1–C3–N3	177.19(17)°	177.27(17)°	177.4(2)°	177.7(3)°
C1–M1–C2	89.35(9)°	89.40(9)°	89.23(11)°	89.41(18)°
C1–M1–C3	89.59(8)°	89.77(8)°	89.24(11)°	89.81(16)°
C2–M1–C3	89.08(8)°	89.14(8)°	89.00(10)	88.94(15)°
M1–Eu1 distance	5.447 Å	5.449 Å	5.455 Å	5.457 Å
Details of $[Eu^{III}(3\text{-pyridone})_2(H_2O)_4(NC)_2]^+$ complexes				
Parameter	**7** (M = $Co_{0.75}Fe_{0.25}$)	**8** (M = $Co_{0.5}Fe_{0.5}$)	**9** (M = $Co_{0.25}Fe_{0.75}$)	**10** (M = Fe)
Eu1–N3	2.5657(16) Å	2.5620(16) Å	2.563(2) Å	2.561(4) Å
Eu1–O1	2.4273(15) Å	2.4273(15) Å	2.4278(18) Å	2.434(3) Å
Eu1–O2	2.4633(14) Å	2.4615(15) Å	2.4636(18) Å	2.467(3) Å
Eu1–O3	2.2988(13) Å	2.2963(13) Å	2.2986(17) Å	2.304(3) Å
Eu1–N3–C3	152.82(15)°	152.66(15)°	152.35(19)°	152.3(3)°
Eu1–O3–C4	134.26(11)°	134.29(12)°	134.10(15)°	134.1(3)°
N3–Eu1–N3	78.33(8)°	78.29(8)°	78.19(10)°	78.14(16)°
O1–Eu1–O1	144.11(7)°	144.32(7)°	144.31(9)°	144.55(14)°
O2–Eu1–O2	70.36(7)°	70.40(7)°	70.26(9)	70.21(13)°
O3–Eu1–O3	149.55(7)°	149.70(7)°	149.79(9)°	149.77(14)°
N3–Eu1–O1	68.78(5)° 147.11(5)°	68.70(5)° 146.98(5)°	68.75(7)° 146.94(7)°	68.65(11)° 146.80(11)°
N3–Eu1–O2	127.70(5)° 130.99(5)°	127.67(5)° 131.02(5)°	127.80(7)° 131.04(7)°	127.71(11)° 131.19(11)°
N3–Eu1–O3	75.24(5)° 81.23(5)°	75.37(5)° 81.21(5)°	75.37(7)° 81.26(7)°	75.37(11)° 81.24(11)°
O1–Eu1–O2	73.27(5)° 77.54(5)°	73.33(6)° 77.66(5)°	73.42(7)° 77.54(7)°	73.40(11)° 77.74(11)°
O1–Eu1–O3	90.48(5)° 98.82(5)°	90.52(6)° 98.69(6)°	90.40(7)° 98.79(7)°	90.32(12)° 98.81(12)°
O2–Eu1–O3	70.40(5)° 139.88(5)°	70.30(5)° 139.83(5)°	70.32(6)° 139.73(6)°	70.37(10)° 139.68(10)°

Table S7. Results of Continuous Shape Measure Analysis for $[Eu^{III}(3\text{-pyridone})_2(H_2O)_4(NC)_2]^+$ complexes in the crystal structures of **1**–**10**.

Compound	CSM parameters			Geometry
	BTP-8	SAPR-8	DD-8	
1	2.479	2.367	0.601	DD-8
2	2.468	2.374	0.590	DD-8
3	2.485	2.388	0.599	DD-8
4	2.471	2.381	0.586	DD-8
5	2.473	2.376	0.602	DD-8
6	2.463	2.358	0.594	DD-8
7	2.460	2.360	0.597	DD-8
8	2.465	2.372	0.601	DD-8
9	2.452	2.361	0.602	DD-8
10	2.437	2.337	0.606	DD-8

* CSM parameters:[S3]
CSM BTP-8 = the parameter related to the bicapped trigonal prism geometry (C_{2v} symmetry)
CSM SAPR-8 = the parameter related to the square antiprism (D_{4d} symmetry)
CSM DD-8 = the parameter related to the dodecahedron (D_{2d} symmetry)
CSM = 0 for the ideal geometry and the increase of CSM parameter corresponds to the increasing distortion from ideal polyhedron.

Table S8. Detailed interatomic distances of hydrogen bonds network of **1**, **2**, and **3**.

Hydrogen bonds	**1**	**2**	**3**
interchain O3-(H4)-N4	2.859 Å	2.857 Å	2.858 Å
interchain O2-(H2B)-N2	2.831 Å	2.835 Å	2.829 Å
interchain O1-(H1A)-N1	3.386 Å	3.387 Å	3.386 Å
intrachain O1-(H1B)-N1	2.747 Å	2.752 Å	2.749 Å
chain to crystallization water O2-(H2A)-O4	2.835 Å	2.841 Å	2.836 Å
chain to crystallization water O4-(H4A)-N3	3.242 Å	3.239 Å	3.239 Å

Table S9. Detailed interatomic distances of hydrogen bonds network of **4**, **5** and **6**.

Hydrogen bonds	**4**	**5**	**6**
interchain O3-(H4)-N4	2.865 Å	2.859 Å	2.859 Å
interchain O2-(H2B)-N2	2.829 Å	2.829 Å	2.829 Å
interchain O1-(H1A)-N1	3.387 Å	3.390 Å	3.390 Å
intrachain O1-(H1B)-N1	2.749 Å	2.748 Å	2.750 Å
chain to crystallization water O2-(H2A)-O4	2.835 Å	2.834 Å	2.835 Å
chain to crystallization water O4-(H4A)-N3	3.245 Å	3.240 Å	3.246 Å

Table S10. Detailed interatomic distances of hydrogen bonds network of **7**, **8**, **9** and **10**.

Hydrogen bonds	**7**	**8**	**9**	**10**
interchain O3-(H4)-N4	2.857 Å	2.855 Å	2.851 Å	2.848 Å
interchain O2-(H2B)-N2	2.826 Å	2.829 Å	2.821 Å	2.831 Å
interchain O1-(H1A)-N1	3.392 Å	3.392 Å	3.400 Å	3.393 Å
intrachain O1-(H1B)-N1	2.750 Å	2.746 Å	2.741 Å	2.747 Å
chain to crystallization water O2-(H2A)-O4	2.836 Å	2.837 Å	2.836 Å	2.841 Å
chain to crystallization water O4-(H4A)-N3	3.244 Å	3.238 Å	3.237 Å	3.227 Å

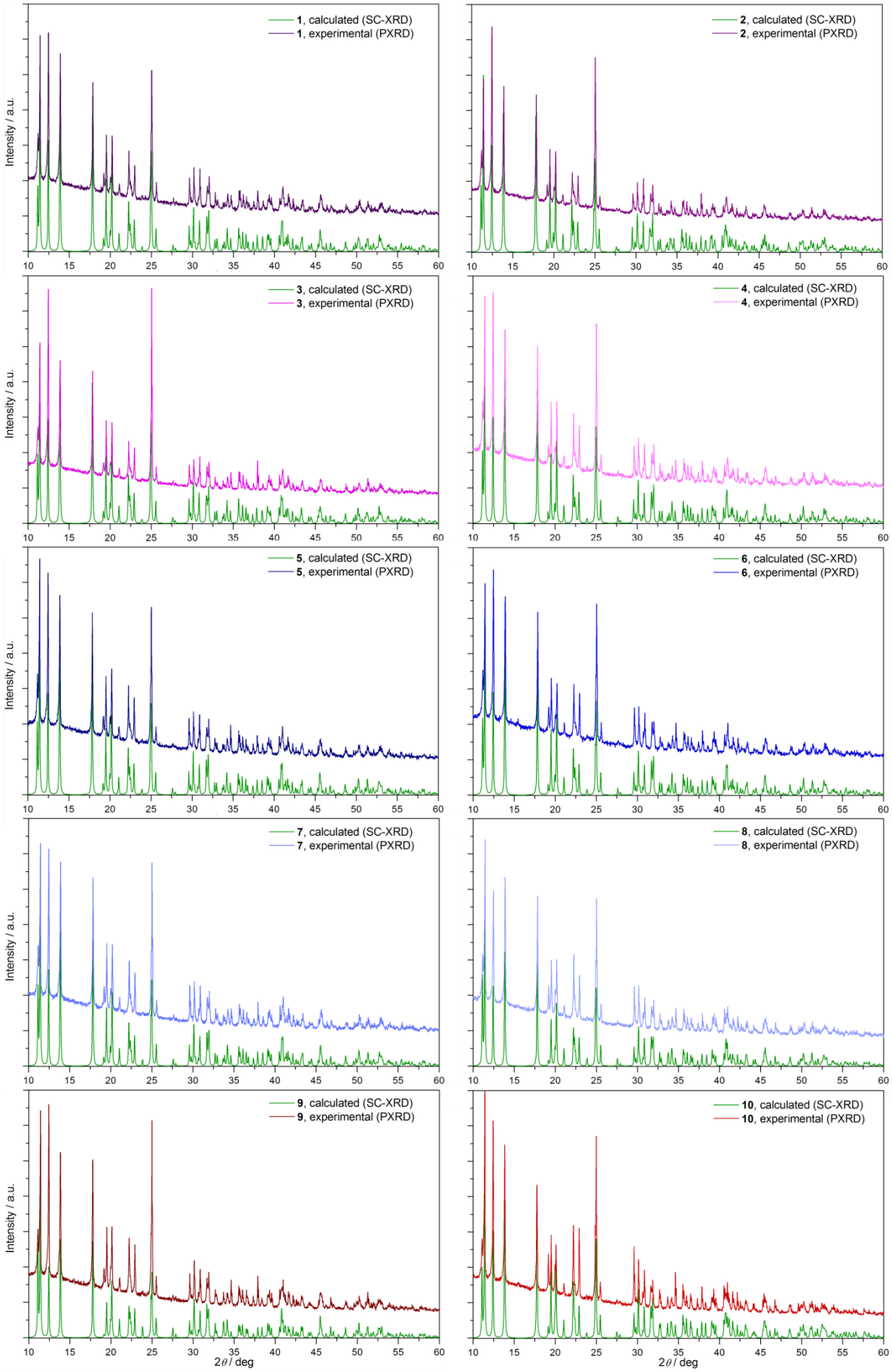

Figure S6. Experimental PXRD patterns of **1–10** compared with the respective patterns calculated from the structural models obtained within the single crystal X-ray diffraction (SC-XRD) structural analyses.

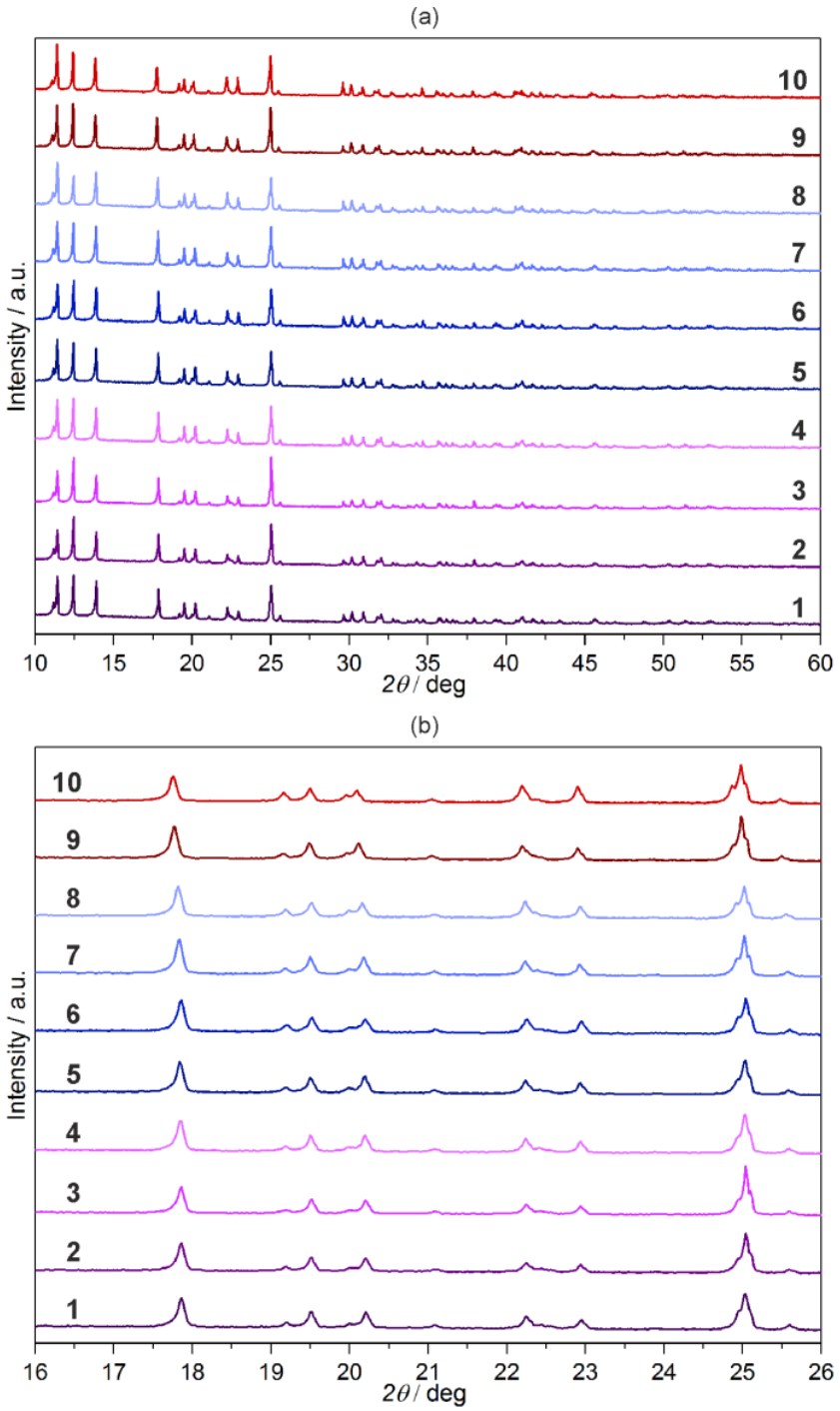

Figure S7. Comparison of experimental powder X-ray diffraction patterns of **1**–**10** (*a*) along with the enlargement of the representative 2*Θ* range of 16–26° (*b*).

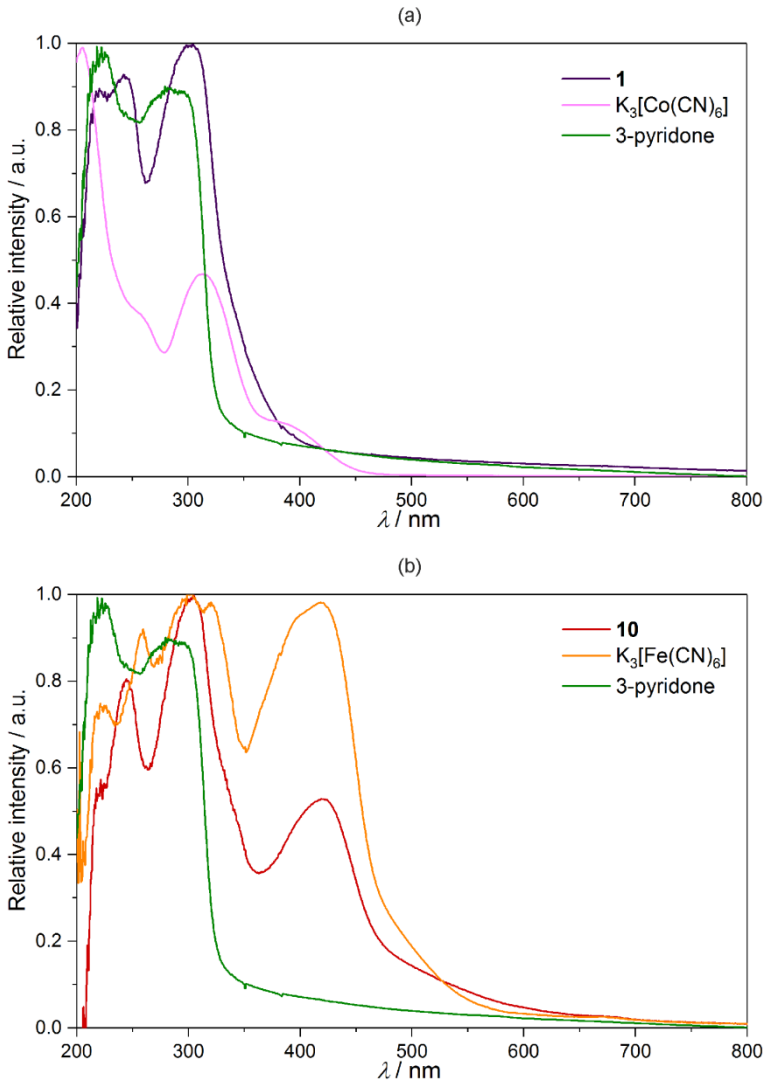

Figure S8. Solid-state UV-Vis-NIR absorption spectra of **1** (*a*) and **10** (*b*) compared with the reference spectra of $K_3[Co(CN)_6]$, 3-pyridone (*a*), and $K_3[Fe(CN)_6]$, 3-pyridone (*b*).

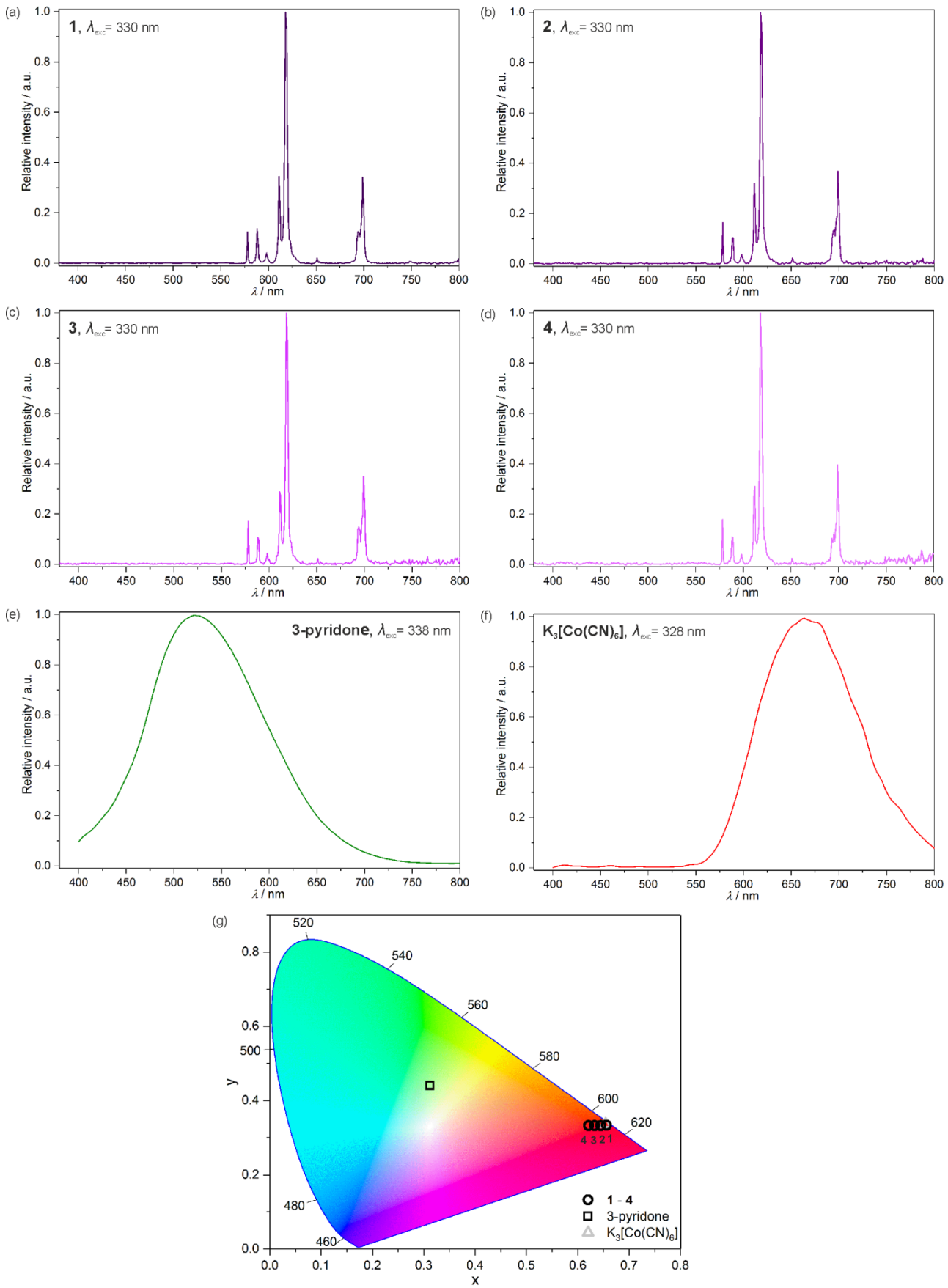

Figure S9. Room temperature solid-state UV-Vis-NIR emission spectra of **1** (*a*), **2** (*b*), **3** (*c*), **4** (*d*), 3-pyridone (*e*), and $K_3[Co(CN)_6]$ (*f*) at the indicated excitation wavelengths together with the related emission colours presented on the CIE 1931 chromaticity diagram (*g*).

Table S11. Summary of *xy* parameters of the CIE 1931 chromaticity scale for the room temperature emission colours of **1**, **2**, **3**, **4**, 3-pyridone, and $K_3[Co(CN)_6]$.

Compound	λ_{exc} / nm	**x**	**y**	**colour**
1	330	0.656	0.334	red
2	330	0.645	0.333	red
3	330	0.633	0.333	red
4	330	0.621	0.333	red
3-pyridone	338	0.312	0.441	green
$K_3[Co(CN)_6]$	328	0.654	0.337	red

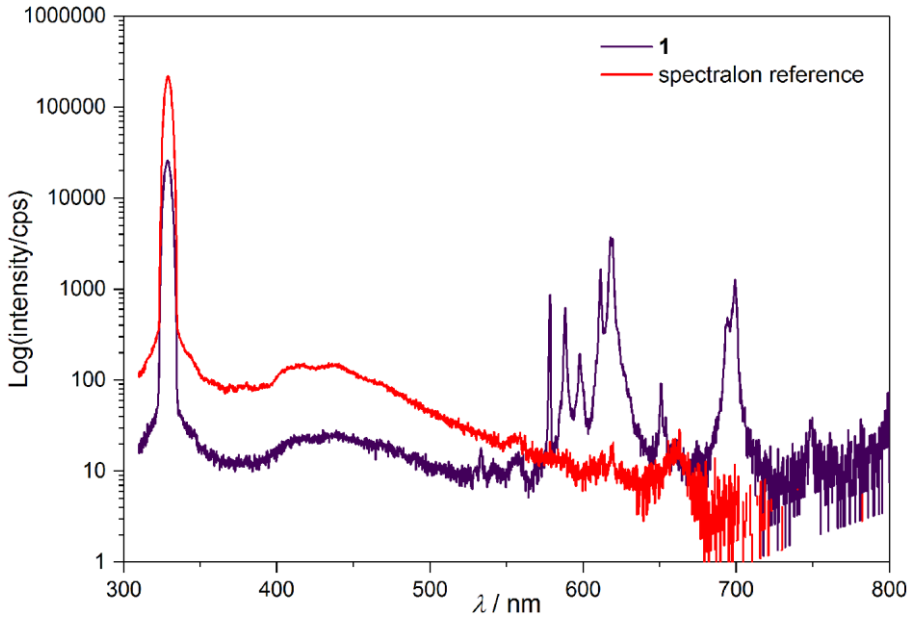

Figure S10. Emission spectra of **1** and the spectralon-made reference used in the calculations of emission quantum yield. The experimental parameters used in the quantum yield determination: excitation wavelength, 330 nm; excitation slit, 5 nm, emission slit, 0.4 nm.

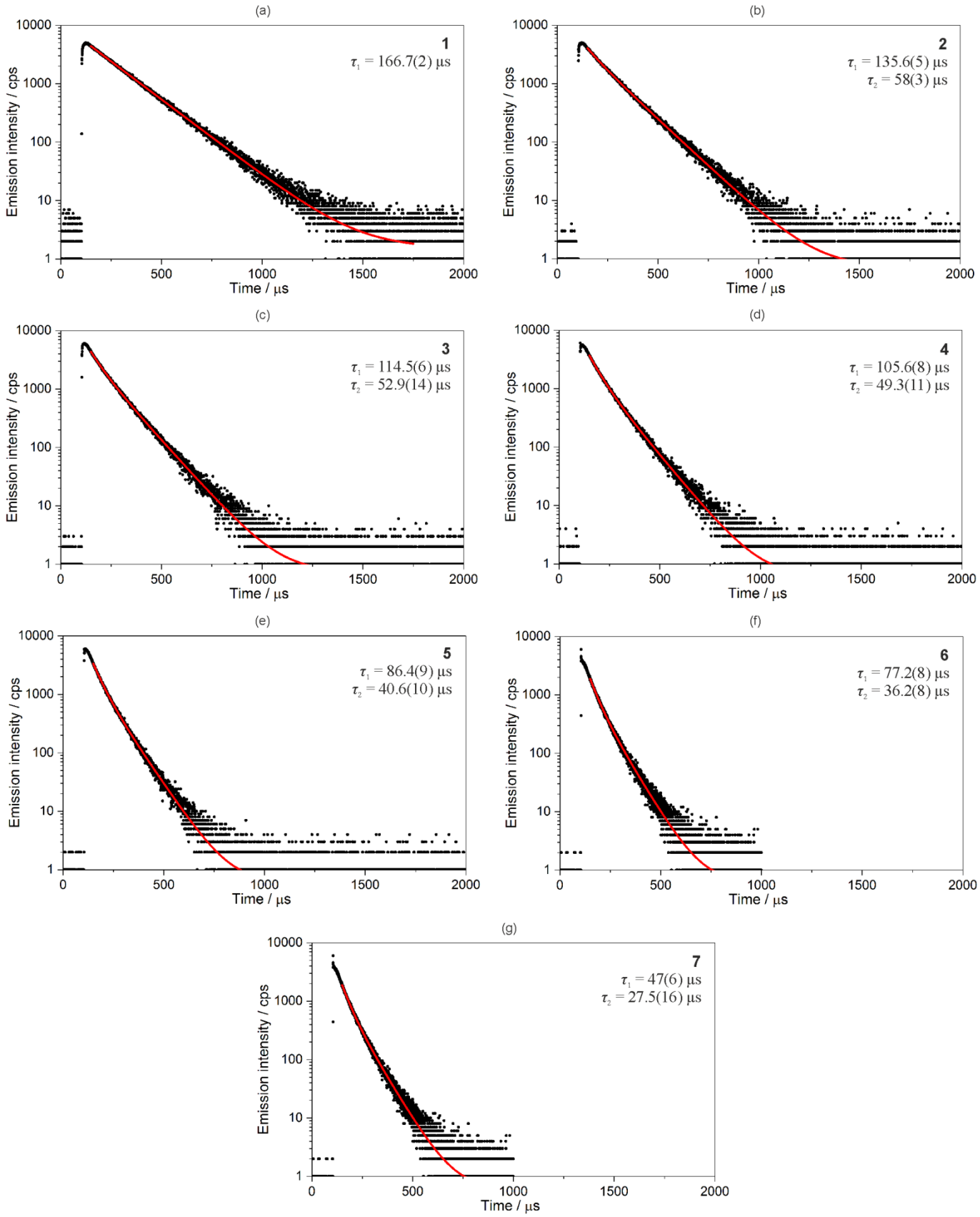

Figure S11. Emission decay profiles of **1** (*a*), **2** (*b*), **3** (*c*), **4** (*d*), **5** (*e*), **6** (*f*), and **7** (*g*) under λ_{exc} = 330 nm and λ_{em} = 618 nm. The black points represent the experimental data while the red lines show the fitting using the mono-exponential (*a*) or double-exponential (*b-g*) decay functions. The resulting emission lifetimes are depicted on the graphs. The detailed parameters, and the related equations are collected in Table S9.

Table S12. Detailed parameters of the fittings of the emission decay profiles of **1**–**7** to the mono-exponential (**1**) and double-exponential (**2**–**7**) decay functions.

compound	τ_1 / μs	τ_2 / μs	B_1	B_2	relative intensity of component **1**	relative intensity of component **2**	χ^2 of the fitting
1	166.7(2)	-	4407(5)	-	100%	-	1.068
2	135.6(5)	58(3)	3273(44)	811(40)	90.4%	9.6%	0.992
3	114.5(6)	52.9(14)	2826(57)	1545(53)	79.8%	20.2%	1.004
4	105.6(8)	49.3(11)	1992(56)	1740(52)	71.0%	29.0%	1.009
5	86.4(9)	40.6(10)	1677(62)	1694(58)	67.8%	32.2%	0.996
6	77.2(8)	36.2(8)	891(34)	1004(32)	65.4%	34.6%	1.018
7	47(6)	27.5(16)	57(2)	114(4)	45.9%	54.1%	0.985

Mono-exponential decay function used for the fitting of the emission versus time curve for **1**:

$$Emission\ intensity\ at\ 618\ nm\ (time, t) = B_1 \cdot \exp\left(-t/\tau_1\right)$$

where τ_1 = emission lifetime.

Double-exponential decay function used for the fitting of the emission versus time curves for **2**–**7**:

$$Emission\ intensity\ at\ 618\ nm\ (time, t) = B_1 \cdot \exp\left(-t/\tau_1\right) + B_2 \cdot \exp\left(-t/\tau_2\right)$$

where τ_1 = first component emission lifetime; τ_2 = second component emission lifetime.

References to Supporting Information

[S1] (*a*) P. Przychodzeń, T. Korzeniak, R. Podgajny and B. Sieklucka, *Coord. Chem. Rev*., 2006, **250**, 2234; (*b*) H. Tokoro, K. Nakagawa, K. Imoto, F. Hakoe and S. Ohkoshi, *Chem. Mater*., 2012, **24**, 1324.

[S2] (*a*) S. Chorazy, K. Nakabayashi, M. Arczyński, R. Pełka, S. Ohkoshi and B. Sieklucka, *Chem. Eur. J*., 2014, **20**, 7144; (*b*) S. Chorazy, M. Rams, M. Wyczesany, K. Nakabayashi, S. Ohkoshi and B. Sieklucka, *CrystEngComm*, 2018, **20**, 1271.

[S3] (*a*) M. Llunell, D. Casanova, J. Cirera, J. Bofill, P. Alemany, S. Alvarez, M. Pinsky, D. Avnir, *SHAPE v. 2.1. Program for the Calculation of Continuous Shape Measures of Polygonal and Polyhedral Molecular Fragments*, University of Barcelona: Barcelona, Spain, 2013; (*b*) D. Casanova, J. Cirera, M. Llunell, P. Alemany, D. Avnir and S. Alvarez, *J. Am. Chem. Soc*., 2004, **126**, 1755.